

Cryo-EM Asymmetric Reconstruction of Bacteriophage P22 Reveals Organization of its DNA Packaging and Infecting Machinery

Juan Chang,^{1,2} Peter Weigele,³ Jonathan King,³
Wah Chiu,^{1,2,*} and Wen Jiang⁴

¹ Graduate Program in Structural and Computational
Biology and Molecular Biophysics

² National Center for Macromolecular Imaging
Verna and Marrs McLean Department of Biochemistry
and Molecular Biology

Baylor College of Medicine
Houston, Texas 77030

³ Department of Biology
Massachusetts Institute of Technology
Cambridge, Massachusetts 02139

⁴ Department of Biological Sciences
Purdue University
West Lafayette, Indiana 47907

Summary

The mechanisms by which most double-stranded DNA viruses package and release their genomic DNA are not fully understood. Single particle cryo-electron microscopy and asymmetric 3D reconstruction reveal the organization of the complete bacteriophage P22 virion, including the protein channel through which DNA is first packaged and later ejected. This channel is formed by a dodecamer of portal proteins and sealed by a tail hub consisting of two stacked barrels capped by a protein needle. Six trimeric tailspikes attached around this tail hub are kinked, suggesting a functional hinge that may be used to trigger DNA release. Inside the capsid, the portal's central channel is plugged by densities interpreted as pilot/injection proteins. A short rod-like density near these proteins may be the terminal segment of the dsDNA genome. The coaxially packed DNA genome is encapsidated by the icosahedral shell. This complete structure unifies various biochemical, genetic, and crystallographic data of its components from the past several decades.

Introduction

The *Salmonella* bacteriophage P22 is a short-tailed double-stranded DNA (dsDNA) phage. The assembly pathway of P22 is well understood and shares a similar assembly and maturation process as tailed dsDNA phages (Prevelige, 2006) and Herpesvirus (Rixon and Chiu, 2003). In this common assembly and maturation process, a procapsid containing scaffolding subunits, but empty of DNA, is formed (Thuman-Commike et al., 1996). A ~43 kb segment of DNA is pumped into the procapsid through the portal complex located at 1 of 12 5-fold vertices (reviewed in Casjens and Weigele, 2005). This DNA packaging is carried out by a terminase-portal complex in an ATP-dependent process (Jardine and Anderson, 2006) utilizing a concatemeric

DNA substrate (Casjens et al., 1992a). The protein complex at the unique packaging vertex in the mature virion is the focal point for the multiple stages in this dynamic process. For P22 (Table 1), the gp7, gp16, and gp20 pilot/injection proteins, together with portal subunits (gp1), are assembled into the procapsid prior to DNA packaging. After DNA packaging, the tail proteins gp4, gp10, and gp26 close up the portal channel. Assembly of the tailspike adhesin (gp9) is the last step in assembly and is required to generate infectious particles. Upon interaction of the tailspikes with the host cell surface lipopolysaccharide (LPS), a rearrangement of these proteins must occur to allow the DNA to exit the virion and cross the cell envelope into the host cytoplasm. The first step in understanding these processes is to obtain a complete picture of the organization of the proteins at the tail vertex.

The icosahedral shell structures of both the procapsid and the infectious phage particles have been extensively studied and solved to subnanometer resolutions using single particle cryo-electron microscopy (cryo-EM) and 3D reconstruction (Jiang et al., 2003). The capsid protein (gp5) was found to share a common fold among dsDNA tailed phages and Herpesvirus (Baker et al., 2005; Bamford et al., 2005). Structural information is available for some of the isolated components, such as cryo-EM reconstructions of the portal dodecamer at 8 Å resolution (Tang et al., 2005) and the tail complex at 27 Å resolution (Tang et al., 2005) and crystal structures of the tailspike's head binding (PDB ID: 1LKT) (Steinbacher et al., 1997) and receptor binding domains (PDB ID: 1TSP) (Steinbacher et al., 1994). X-ray solution scattering has also been used to characterize the conformation of the condensed dsDNA (Earnshaw and Harrison, 1977). However, due to the absence of a complete structure of the entire infectious phage particle, many questions remain about how these distinct components interact and form such a nanomachine.

The lack of a complete structure of P22 is due to the limitations of traditional structural methods (both X-ray crystallography and single particle cryo-EM), which rely on symmetry averaging and thus can only resolve the structure of the major component, the icosahedral shell. Recently, methods have been introduced to reconstruct spherical viruses without icosahedral averaging, and they have been used to determine the structures of phages T7 (Agirrezabala et al., 2005) and Epsilon15 (Jiang et al., 2006). In this study, we have applied the asymmetric reconstruction method to determine the entire structure of the P22 infectious particle, revealing the structural anatomy of its molecular components. The complete P22 virion structure will be discussed in the context of assembly and infection as well as compared to the equivalent structural features found in bacteriophages Epsilon15 and T7.

Results

Figure 1 shows a cryo-EM image of infectious P22 particles. The ~700 Å diameter particles are angular in

*Correspondence: wah@bcm.tmc.edu

Table 1. Structural Components in the Infectious P22 Phage Particle

Protein	Copies	Location	Function	Structure
gp1	12	Portal	dsDNA packaging and release	This paper; Bazinet et al., 1988; Tang et al., 2005
gp4	12(?)	Tail hub	Head completion	This paper; Tang et al., 2005
gp5	415	Shell	Capsid shell	This paper; Jiang et al., 2003; Prasad et al., 1993; Thuman-Commike et al., 1996; Zhang et al., 2000
gp7	?	Portal central channel	Infection	This paper
gp9	6 × 3	Tailspike	Host recognition	This paper; Steinbacher et al., 1994, 1997; Tang et al., 2005
gp10	6	Tail hub	Head completion	This paper; Tang et al., 2005
gp16	?	Portal central channel	Infection	This paper
gp20	?	Portal central channel	Infection	This paper
gp26	3	Tail needle	Genome stabilization; Host cell penetration	This paper; Tang et al., 2005
dsDNA	43 kb	Capsid chamber	Genetic information	This paper

profile and filled with dsDNA. A tail appendage can be discerned at the edge of the capsid for some particles at suitable views. Some views show the 6-fold nature of the tail. Approximately 19,000 particle images were recorded and used to determine the entire structure of the infectious phage particles. The particle images were initially processed using the classic icosahedral averaging method and then further processed to relax the symmetry assumption entirely. The final 3D reconstruction without symmetry imposition is shown in Figure 2A and Movie S1 (see the Supplemental Data available with this article online). Figures 2B and 2C shows the density maps of the mature phage and the procapsid with icosahedral averaging (Jiang et al., 2003) filtered at equivalent resolution as the infectious particle for comparison. A significant conformational change in the hexon subunit arrangement occurs during DNA packaging, as seen in these maps and reported previously (Jiang et al., 2003; Prasad et al., 1993).

Capsid Shell

The capsid shell component of the 20 Å resolution density map in this asymmetric reconstruction (Figure 2A) is nearly identical to that derived using the classic icosahedral reconstruction (Jiang et al., 2003) at similar resolution (Figure 2B) except for a unique vertex where the tail is attached. Due to icosahedral symmetry imposition, all the nonicosahedral components are averaged away and not visible in the classic icosahedral reconstruction (Figure 2B). The asymmetric reconstruction shows distinct surface features such as hexons and pentons in the icosahedral shell. However, since one penton is replaced by the portal dodecamer (see below), it appears that the shell is composed of 415 copies of gp5 protein arranged in a T = 7 *laevo* icosahedral lattice. This type of capsid symmetry is a conserved feature among many of the tailed dsDNA phages such as T7 (Steven et al., 1983), P2 (Dokland et al., 1992), lambda (Dokland and Murialdo, 1993), SPP1 (Droge et al., 2000), HK97 (Wikoff et al., 2000), and Epsilon15 (Jiang

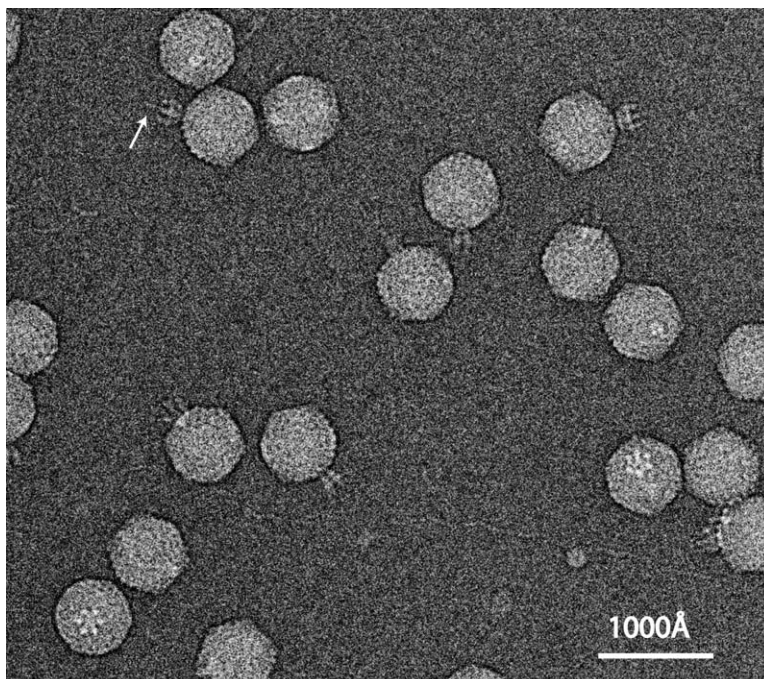


Figure 1. A 200 kV CCD Image of the Bacteriophage P22 Infectious Particles Embedded in Vitreous Ice
Some views show a 6-fold tail or the “needle” (arrow).

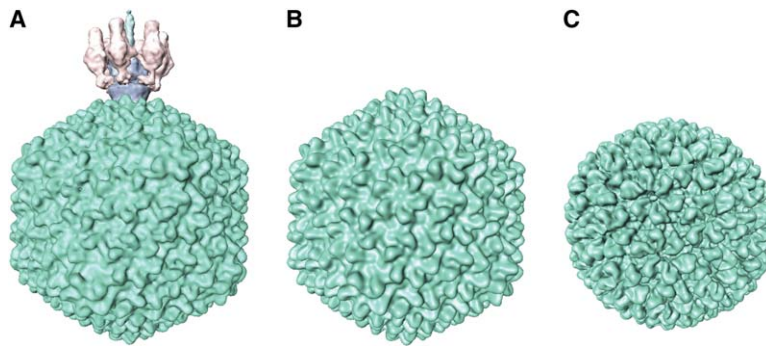


Figure 2. Surface Rendering of Density Maps of Bacteriophage P22 Based on Different Reconstruction Methods

(A) An asymmetric reconstruction of infectious particle and (B–C) an icosahedral reconstruction of the infectious particle and the procapsid particle determined previously (Jiang et al., 2003) and filtered to similar resolutions for comparison. The hexons are skewed about a pseudo-2-fold axis in the procapsid and become more 6-fold-symmetric in the infectious particle.

et al., 2006). The shell is angular with a vertex-to-vertex distance of ~ 700 Å and a face-to-face distance of ~ 650 Å, which are in agreement with the measurements from X-ray solution scattering (Earnshaw and Harrison, 1977). The excellent agreement of the shell structure derived in the asymmetric reconstruction with that from the long-established icosahedral reconstruction validates the correctness of the asymmetric reconstruction. The individual structural components in the asymmetric reconstruction are segmented and annotated in the sectional and cutaway views as shown in Figure 3.

Tail Complex

The tail complex is located at 1 of the 12 icosahedral 5-fold vertices and consists of the tail hub, tailspikes, and the tail needle (Figures 2A and 3; Movie S1). The shell-proximal region of the tail complex contacts/interacts with the portal complex and possibly the neighboring capsid proteins. The distal regions of the tail complex, including the tailspikes, are used to attach the virus to its host's surface.

A tubular tail hub (Botstein et al., 1973; King et al., 1973; Poteete and King, 1977; Strauss and King, 1984) is attached to the external side of the portal vertex (Figure 3 and Movie S1). The tail hub can be roughly divided into two stacked barrels (Figure 4A), with the portal/shell proximal barrel and the distal barrel showing six bulges (Figure 4B). It has been shown that the tail hub is composed of gp4 and gp10. During assembly, gp4 binds to the capsid first, followed by gp10 (Botstein et al., 1973). Thus the density proximal to the capsid shell

and portal was assigned as a ring of gp4, while the distal density was assigned as a hexamer of gp10. The tail hub is filled and seals the capsid (Figure 3 and Movie S1). This agrees well with the role of gp4 and gp10 in keeping the packaged DNA inside the capsid (Strauss and King, 1984).

Attached to the distal end of the tail hub is a long needle (Figure 4A) that can be assigned to a triple-stranded coiled-coil formed by gp26 (Andrews et al., 2005). This rigid tail needle extends significantly further out than the tailspikes (Hartwig et al., 1986) and could function as a host cell surface-penetrating device similar to the bacteriophage T4 baseplate needle (Kanamaru et al., 2002), either by facilitating DNA injection into the host cell or insertion into an outer membrane pore. Its location at the center of the distal end of the tail hub suggests it can also serve as a capping protein to prevent premature leakage of packaged dsDNA (Strauss and King, 1984).

Six trimeric tailspikes bind in a groove at the interface between the gp4 and gp10 layers of the tail hub (Figures 4A and 4B). The arrangement of the six tailspikes around the tail hub is very close to 6-fold symmetric (Figure 4B). Each tailspike is a trimer of the 666 amino acid long gp9. Each tailspike trimer consists of two domains (Figure 4A): the head binding (PDB ID: 1LKT) (Steinbacher et al., 1997) and the receptor binding (PDB ID: 1TSP) (Steinbacher et al., 1994) domains. Each of these domains has been crystallized separately as a trimer with exact or near 3-fold symmetry. The crystal structures of these two domains were fitted into the cryo-EM

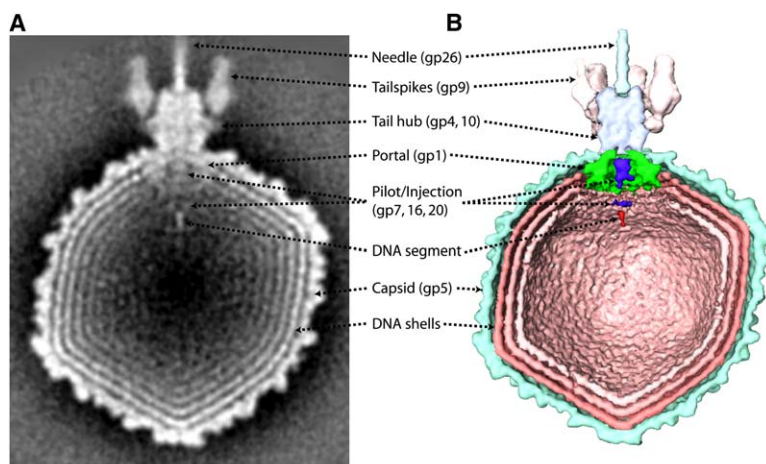


Figure 3. Annotations of the Structural Components of Bacteriophage P22

(A) A central section of the density map. (B) A cut-away isosurface view.

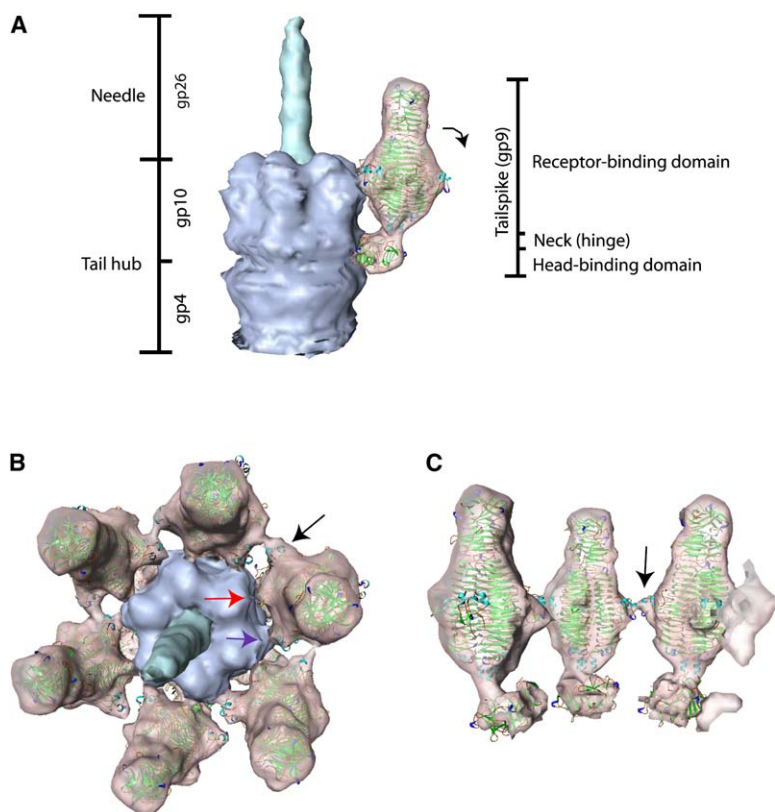


Figure 4. Tailspike Structure and Interactions

The crystal structures of the receptor binding domain (1TSP) and head binding domain (1LKT) of the tailspike are fitted into the cryo-EM map.

(A) The side view of the segmented tail hub and the attachment of a single tailspike at the interface between gp4 and gp10. The neck region between the two domains of the tailspike may bend out (curved arrow) during the infection process.

(B) Top view of the tail needle, tail hub, and tailspikes. Red and purple arrows show the interactions between the tailspike and the hub, while the black arrow shows the interactions between adjacent tailspikes. The α helix protrusion (black arrow) interacts with the adjacent tailspike's LPS binding site area.

(C) Computationally removing the tail hub and half the tailspikes shows the interactions between adjacent tailspikes (black arrow).

maps independently (Figure 4). The head binding domain fits well into the density map. Fitting of the receptor binding domain was not unambiguous. This uncertainty was due to the lack of resolution sufficient to visualize individual subunits of the trimer. Furthermore, the cryo-EM map does not exhibit exact 3-fold symmetry in the tailspike's receptor binding domain. Also, two similarly sized protrusions per subunit near the LPS binding site (middle of this domain) are spaced azimuthally 60° apart (red and purple arrows in Figure 4B). Thus there are two plausible fits that are spaced 60° apart around the tailspike symmetry axis. However, in either of the two fits, the loops (red arrow) and short α helices (purple arrow) contact the distal end of the tail hub (Figure 4B). One possible fit is shown in Figure 4B, in which the indentation in the tailspike between the α helix and loop protrusions (black and red arrows, respectively) corresponds to one LPS binding site. The two other LPS binding sites are spaced 120° away. As a result, two LPS binding sites in this conformational state are facing either the tail hub or adjacent tailspikes and are hidden, while only one site is exposed to the outside. In the alternative fit, the inter-tailspike interaction sites would be between the small loop on one tailspike and the cleft of two adjacent subunits in the neighboring tailspike. In this alternative model, two LPS binding sites would be facing outside.

In the virion bound tailspike, the two domains are connected by a narrow neck clearly seen in our cryo-EM map (Figure 4A), likely composed of an α -helical trimeric coiled-coil (Steinbacher et al., 1997). The neck region is the first part of the protein susceptible to cleavage by proteases in the presence of heat and detergent, sug-

gesting it has some flexibility (Chen and King, 1991; Steinbacher et al., 1994). In the cryo-EM map, the quasi-3-fold axes of these two domains are not aligned. In fact, there is a $\sim 6^\circ$ inclination between the quasi-3-fold axes of these two domains, resulting in a kink between these two domains. A possible role of this kink, as well as the roles of tailspike-tailspike and tailspike-hub contacts, in the process of DNA ejection is discussed below.

Portal

The portal, composed of 12 copies of gp1 (Bazin et al., 1988), is located underneath the tail hub (Figure 3 and Movie S1). Together with the large and small terminase subunits (gp2 and gp3, respectively), the portal functions as part of a powerful molecular motor responsible for packaging the dsDNA genome into the capsid cavity, as elucidated in the phi29 phage system (Smith et al., 2001). The terminase proteins, which temporarily associate with the portal during DNA packaging, dissociate from the virion intermediately after completion of packaging and are not found in the virion (Casjens and Hayden, 1988).

The P22 portal complex is cone shaped, with the narrower (~ 110 Å) stalk domain and wider wing (~ 170 Å) and crown domains (~ 150 Å) (Figure 5A). The central channel of the portal also varies in size, with the narrowest part (~ 25 Å) at the opening of stalk domain. This size agrees well with the role of the portal as the conduit for dsDNA. Structural analyses of biochemically purified portal complex of other dsDNA viruses have shown them to exist in a mixture of oligomeric conformations in solution (Cingolani et al., 2002; Orlova et al., 2003;

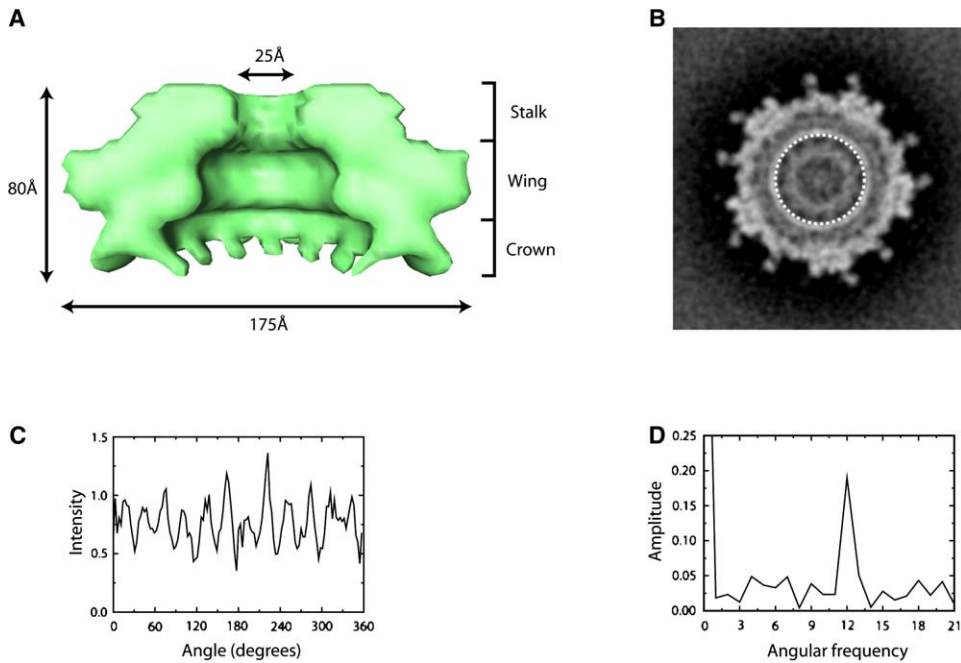


Figure 5. Portal Structure

(A) A cutaway side view of the 12-fold averaged portal shows three morphological domains: stalk, wing, and crown.

(B) A slice through the density of the unaveraged portal region shows 12 spokes.

(C and D) An azimuthal density distribution plot (C) of the circled region in the radii range 25–95 Å in (B). Its power spectrum shows a peak at 12 (D).

Trus et al., 2004). A slice through the 3D density segments of the portal, its azimuthal density plot, and corresponding power spectrum unambiguously demonstrate 12 “spokes” (Figures 5B–5D). The same stoichiometry is also found in the portal protein in T7 (Agirrezabala et al., 2005) and Epsilon15 particles (Jiang et al., 2006).

Pilot/Injection Proteins

Additional protein-like densities fill the channel spanning the tail hub and portal complex (Figure 3 and Movie S1). Table 1 lists the nine proteins that make up the infectious capsid (Botstein et al., 1973; King et al., 1973, 1976). With all the structural proteins assigned, this leaves the pilot/injection proteins gp7, gp16, and gp20 to account for the densities located in the portal channel. However, the channel of the tail hub appears to be occupied with densities that could be either pilot/injection proteins protruding from interior through the portal channel or the hub proteins (gp4, gp10) in a closed conformation. The pilot/injection proteins have been shown to be essential in infection (Poteete and King, 1977). Gp16 enters the cytoplasm in the early stages of infection (Bryant and King, 1984; Hoffman and Levine, 1975a). The location of the pilot/injection proteins at the opening to the portal channel, as suggested in this reconstruction, would position the pilot/injection proteins for entry into the cytoplasm along with the phage DNA during infection.

Unlike bacteriophage Epsilon15 (Jiang et al., 2006) or T7 (Agirrezabala et al., 2005), P22 does not have a large internal protein core encircling a terminal segment of DNA. Instead, a small ring-like density (Figure 3) between the DNA fragment (see below) and the portal

was present, which could be gp7, gp16, or gp20. Its location suggests that this small cluster of proteins may lead the DNA during exit into the cytoplasm.

DNA Packing

Overall, the DNA appears as concentric shells. The three outermost layers of dsDNA can be seen in the capsid (Figure 6 and Movie S1). The outermost layer and the

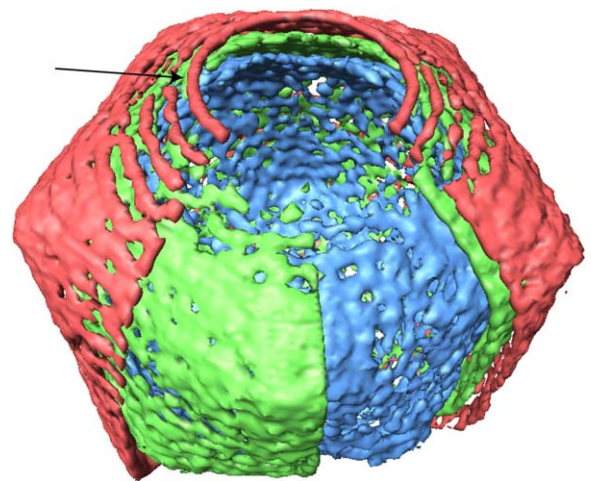


Figure 6. The Layers of dsDNA Segmented from the 3D Map are Coaxially Packed around the Tail/Portal/Capsid Axis

The order is better in the outermost layer and in the region near the portal, but there is more disorder in the inner layers. A ring of clearly defined density surrounds the portal wing domain (arrow).

region near the tail/portal are the best resolved and display coaxial packing (Figures 3 and 6). The inner layers are less ordered and have weaker densities. The distance between layers is measured to be 21–24 Å, which is in agreement with the broad peak seen in X-ray solution scattering (Earnshaw and Harrison, 1977; Thuman-Commike et al., 1999).

One of the internal structures that can be visualized is a short, cylindrical density near the center of the capsid (Figure 3). Due to its high-density value, this was interpreted as a terminal segment of dsDNA. Its position suggests that it is primed to exit the capsid through the portal. As a result, this fragment may be the last DNA that was packaged into the capsid, and the first to be released upon infection. This is reminiscent of the similarly positioned terminal segment of dsDNA in Epsilon15 (Jiang et al., 2006). However, there is a significant difference in the length of the visible terminal segment of dsDNA in P22 and the ~90 bp terminal segment of dsDNA in Epsilon15.

Discussion

Comparison with Bacteriophages Epsilon15 and T7

Asymmetric reconstruction offers the opportunity of seeing those structural components of the spherical viruses that are invariant from particles to particle. If the structural components varied from particles to particle, they would not be resolved using the current methodology. Asymmetric reconstructions were previously reported for bacteriophages T7 (Agirrezabala et al., 2005) and Epsilon15 (Jiang et al., 2006).

The asymmetric reconstruction of the whole P22 virion compared to those of Epsilon15 and T7 reveals an overall structural similarity among them, but with key differences. The mature phages have similar capsid dimensions (~700 Å in diameter). P22 packages ~3 kb more DNA than Epsilon15 (McConnell et al., 1992) and T7 (Cerritelli et al., 1997). Assuming the volume inside the shell and the DNA packing density are the same, the extra space occupied by the significantly larger protein cores in both T7 and Epsilon15 could account for this difference in the larger packaged genome of P22. The DNA terminal segment appears much shorter in P22 and adjoins some protein densities between it and the portal protein. In Epsilon15, the analogous segment of DNA is surrounded by a protein core. A similar protein core surrounding a DNA segment is also seen in bacteriophage T7 (Agirrezabala et al., 2005). Unlike Epsilon15 and T7, the tail hub in P22 appears to be completely filled. These differences probably stem from different mechanisms used by the phages to accomplish the same task: delivering DNA across the tripartite cell wall. This is not surprising since the phages also use totally different proteins to bind LPS.

The attachment apparatus of these phages, though not homologous, accomplishes the same function. Although they have tail hubs external to the portal protein, a needle-like structure is notably absent from Epsilon15 and T7. All have LPS binding tailspikes, but where the adhesins of Epsilon15 deviate significantly from 6-fold symmetry, the P22 tailspikes are arranged with near-perfect 6-fold symmetry around the tail hub (Figure 4 and Movie S1). Tail fibers are not seen in the asymmetric reconstruc-

tion of the T7 virion (Agirrezabala et al., 2005). The bacteriophage P22 tailspike subunit contains a parallel β helix domain, which binds and cleaves the O-antigen component of cell surface lipopolysaccharide. Epsilon15 similarly has “receptor-degrading” activity (Hoffman and Levine, 1975b); however, its tailspike is probably a β propeller domain, similar to that seen for the capsule-degrading coliphage K1F (Stummeyer et al., 2005). K1F tailspike has a similar three-lobed, club-shaped end as the tailspike of Epsilon15. In contrast, the T7 tail fibers are much more slender coiled-coils and do not appear to have enzymatic activity (Steven et al., 1988).

How Is the Virion Built?

The virion is but one step in a dynamic process utilizing a range of assembly intermediates and protein conformations. As shown previously (Jiang et al., 2003; Prasad et al., 1993) and in Figure 2, the icosahedral capsid shell undergoes large conformational changes in the maturation process. The asymmetric reconstruction of the whole virion reveals not only the organization and arrangement of the DNA and all structural proteins, but it also sheds light on the processes of virion assembly and DNA ejection (schematically outlined in Figure 7).

The earliest detectable structure in the P22 assembly pathway is the procapsid, a protein container into which the DNA genome is pumped (Prevelige, 2006). It is composed of a capsid protein shell (gp5), portal proteins (gp1), the pilot/injection proteins (gp7, gp16, and gp20), as well as the internal scaffolding protein (gp8). The scaffolding protein exits the procapsid at around the time of DNA packaging and is not found in the mature virion (King and Casjens, 1974). This protein promotes the rapid and accurate assembly of free capsid subunits into a closed shell (Prevelige et al., 1988). How the procapsid incorporates a single complex of portal protein, as well as the correct complement of pilot/injection proteins, is not known. The portal protein has been shown not to be a kinetic initiator of P22 assembly (Bazin et al., 1988). However, the scaffolding protein has been shown genetically and biochemically to interact with the portal protein as well as gp16 (Greene and King, 1996; Weigele et al., 2005), suggesting a central role for the scaffolding protein in bringing the proteins that make up the injection apparatus together with the capsid subunits. The location of the pilot/injection proteins just interior to the portal complex (Figure 3 and Movie S1) suggests not only that they are conveniently positioned for exiting the capsid during infection, but that they are also spatially close for assembly, as their genetic interaction suggests.

After the procapsid is assembled, DNA is packaged by the portal-terminase complex in an ATP-dependent process. The cutting of the DNA is catalyzed by the terminase complex (gp2/3). The amount of DNA packaged is regulated by the portal protein (Casjens et al., 1992b). DNA is densely packed in the head and requires counter-ions to stabilize it. The DNA surrounding the portal is unusually ordered, forming a clearly defined ring of density around the wing region of the portal dodecamer (Simpson et al., 2000) as seen in Figure 6 (arrow). Interior to this ring are domains of portal protein not observed in the portal protein of phi29 (Simpson et al., 2000). The DNA packing appears more ordered

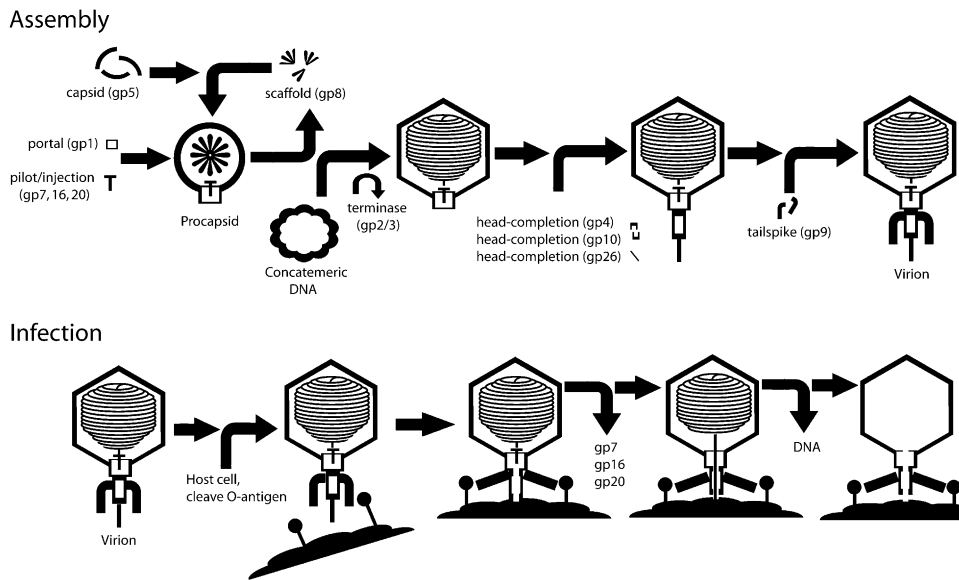


Figure 7. Plausible Model for dsDNA Packaging and Release of Bacteriophage P22

In the assembly process (top row), a procapsid is first formed by portal (gp1), shell (gp5), scaffold (gp8), and pilot/injection (gp7, gp16, and gp20) proteins. Next, terminase (gp2/3), together with portal, packages the DNA into the capsid as scaffold proteins exit. Then, tail hub protein gp4 binds to the portal, followed by additional tail hub protein gp10 and tail needle protein gp26. Binding of tailspike (gp9) completes the virion. During infection (bottom row), tailspikes interact with the host cell surface LPS O-antigen. Digesting this receptor brings the virus nearer to the cell surface. At the same time, the binding signal is transmitted via the tail hub. The tail needle and tail hub proteins then create a channel throughout the outer membrane, peptidoglycan, periplasm, and inner membrane. Finally, the pilot/injection proteins exit the capsid and are injected into host cell cytoplasm, followed by DNA.

at the outer layers and near the portal, as evidenced by the presence of continuous strands of density in these regions (Figure 6 and Movie S1). In the inner regions, the density is discontinuous. The DNA at the outer layer and near the portal can interact with the proteins, while the DNA in the other regions interacts with other DNA. This indicates that the ordering may be the result of DNA-protein interactions. It is worth noting that the packaged genome consists of a single long chain of dsDNA molecule, and a properly resolved structure of the packaged genome should show multiple rounds of a continuous spiral instead of the currently observed multiple disconnected rings for both the P22 and Epsilon15 (Jiang et al., 2006) genomes. It is well known that each P22 particle contains slightly different lengths of DNA (Casjens and Hayden, 1988; Casjens and Weigele, 2005). The currently observed pattern of genome packing may be attributable to the effect of a computational averaging of the dsDNA with slightly different azimuthal orientations in different particles (a total of 16,000 in the asymmetric reconstruction). This type of heterogeneous orientation of the viral genome could be a general feature of the tailed dsDNA phages.

Once DNA is packaged, it must be kept inside the capsid until the initiation of infection. Gp4, gp10, and gp26 close up the portal channel (Figure 3). Particles lacking any of these proteins do not retain their DNA (Strauss and King, 1984). What prevents the premature addition of these proteins to the developing virion? It could possibly be that a conformation of portal protein signals both the cutting of DNA by terminase and the release of terminase from the expanded capsid. Then the portal protein in the packed conformation would present

a competent surface for the binding of gp4. Gp10 and gp26 would then add successively to the nascent tail hub followed by binding of the tailspike homotrimer. A similar sequence of events and structural transitions has been proposed for the maturation of the T7 virion (Agirrezabala et al., 2005).

How Does the Virion Infect?

The virion in its fully assembled state must subsequently undergo conformational changes to allow the passage of DNA through the ejection vertex. In the first step of infection (Figure 7), P22 adsorbs to the O-antigen component of cell surface LPS through its tailspike proteins (Israel et al., 1972). The tailspike has endorhamnosidase activity, which is believed to allow the phage to “chew” its way down to the surface of the host (Iwashita and Kanegasa, 1973). Subsequent steps leading to the delivery of phage DNA across ~260 Å combined thickness of the outer membrane, peptidoglycan, periplasm, and inner membrane into the host’s cytoplasm are still poorly understood. The tailspike, as assembled onto the tail hub, is in a kinked conformation that breaks the 3-fold symmetry of this homotrimer (Figure 4A). The site of this kink forms the neck domain between the head binding domain and the rest of the molecule. The asymmetric reconstruction suggests there are lateral interactions between the tailspike proteins (black arrows in Figures 4B and 4C) as well as interactions between the receptor binding domain and the tail hub (red and purple arrows in Figure 4B). Such interactions might be used to hold the tailspike in a kinked conformation after binding the tail hub during virus assembly. A concerted outward motion of the tailspike domains (arrow in Figure 4A), like the

blooming of a flower (Steinbacher et al., 1997), might act as conformational lever delivering a signal to the gp4, gp10, gp26 complex during infection. In the context of the structure presented here, this motion would transmit a conformational signal to the interface between gp4 and gp10, somehow resulting in the opening of the channel for DNA passage. It is conceivable that the interactions across adjacent tailspikes and between tailspikes and tail hub may be broken and altered during this process.

The structure of the tail vertex suggests additional rearrangements that must occur in order for DNA to exit the capsid. Recent work showing that gp4 has transglycosylase activity leads to the intriguing possibility that this protein can reach peptidoglycan through the outer membrane (Moak and Molineux, 2004). However, from the host cell's perspective, gp4 sits behind a ring of gp10 and the gp26 needle. Therefore, gp10 and gp26 must get out of the way, or dramatically reorganize, before gp4 can reach the membrane. The role of the pilot/injection proteins and ejection of phage DNA is still poorly understood. P22 strains unable to express gp16 (one of the pilot/injection proteins) can adhere to cells, but fail to inject their DNA (Hoffman and Levine, 1975b). However, this block can be relieved by expression of gp16 in *trans*; that is, intracellularly expressed gp16 can complement a virion lacking gp16 and does so from the cytoplasmic side of the inner membrane (Bryant and King, 1984; Hoffman and Levine, 1975b). Therefore, gp16 is important for getting DNA across the inner membrane. In the context of the virion's structure, gp16 (together with the other pilot/injection proteins) is positioned to exit the channel before the DNA. Internal core proteins in bacteriophage T7 have been shown to exit the capsid in the early stages of infection (Kemp et al., 2005), possibly forming an extended channel into the host and suggesting that a similar phenomenon may occur in P22.

It is not known whether LPS with O-antigen is sufficient to allow P22 to infect or if a coreceptor is also required. P22 may use O-antigen in an initial binding and subsequently dock onto a host protein pore or channel, as is the case for phages T5 (Plancon et al., 1997) and lambda (Roessner et al., 1983). Alternatively, P22 may use LPS to access regions of the outer membrane likely to be near the inner membrane. The synthesis of LPS (reviewed in Whitfield, 1995) begins on the inner membrane. Through a series of steps, the core polysaccharide is transferred to the outer membrane, where O-antigen repeats are enzymatically added to a growing oligosaccharide. LPS is probably found in patches on the cell surface, and sites rich in O-antigen synthesis may be regions where the outer and inner membranes are close enough for P22 proteins to span both membranes (Bayer, 1968). Future structural studies of phage particles in the process of binding to the host cell surface and releasing DNA will reveal these processes in greater detail.

Experimental Procedures

Sample Preparation

Mid-log cultures of *Salmonella typhimurium* LT2 were infected with a phage strain defective in lysis (P22 *c1-7*, *13am*) at an MOI of 5. Cultures were incubated with shaking for 90 min at 37°C. Infected cells were pelleted by centrifugation and resuspended in 1/100 volume of buffer TM (10 mM Tris [pH 7.5] and 1 mM MgCl₂). The resuspended

cells were lysed by adding an equal volume of chloroform followed by vigorous vortexing. Lysozyme (1 mg/ml) and DnaseI (10 µg/ml) were added to aid lysis and reduce viscosity. Debris and organic phase were separated by centrifugation. The resulting supernatant containing virions was layered atop 20% sucrose and sedimented through a layer of CsCl rho = 1.4 onto a cushion of CsCl rho = 1.6 in the ultracentrifuge at 100K average RCF for 2 hr at 4°C using an SW50.1 rotor. A visible phage band was harvested using a 20 gauge hypodermic needle and dialyzed against three changes of buffer TM. Using this method, titers of phage greater than 10¹²/ml were routinely obtained.

Cryo-EM

A Vitrobot (<http://vitrobot.com>) was used to flash-freeze a 3 µl aliquot of sample onto a copper Quantifoil R2/2 grid. The sample was loaded onto a Gatan 626 cryoholder and imaged in a JEM 2010F electron cryomicroscope (JEOL USA, Peabody, MA) operated at 200KV and at a specimen temperature near liquid N₂. Using JAMES imaging system (Booth et al., 2004), ~1,200 images were collected on a Gatan 4k CCD, with a dose of 10–15 e/Å² and a defocus of 2–5 µm at a final magnification on CCD ~55,360×. The defocus range of 2–5 µm ensures images with good contrast that were easier to computationally box out and process. The images were immediately archived in the EMEN database (Ludtke et al., 2003) for subsequent processing.

Image Processing

Image processing was performed essentially as previously described (Jiang et al., 2006). About 19,000 particles were selected by first using automated selection by the *ethan* program (Kivioja et al., 2000) and then followed by manual screening using *boxer* in EMAN (Ludtke et al., 1999). In order to expedite the computation, a smaller box size was chosen, even though it slightly truncated the long needle in side views. The box size was large enough to include the six tailspikes. Contrast transfer function parameters of each CCD image were determined using an automated CTF fitting routine (C. Yang et al., personal communication). EMAN was then used to refine and reconstruct the map with icosahedral symmetry imposed (Jiang et al., 2006). The ~16,000 particles included in the final icosahedral reconstruction were then used for further reconstruction without imposing any symmetry.

To avoid any possible initial model bias, the initial model of a tailed capsid was generated by computationally adding a cylindrically symmetrical ring of densities at one of the 5-fold vertices of the icosahedral reconstruction. The tailed model was projected in the 60 equivalent views of icosahedral symmetry and compared with the raw particle image to identify the best matching view for each of the particle images. These orientations were used to reconstruct the map without imposing any symmetry. This process was iterated until the cylindrical symmetry of the tail was gradually broken and converged to reveal a tail with six tailspikes and a dodecameric portal. This type of two-stage processing is required since direct one-stage refinement with C1 symmetry failed to resolve those non-icosahedral components. The final resolution of the asymmetric reconstruction is at ~20 Å as judged by Fourier shell correlation (Harauz and van Heel, 1986) of two half dataset reconstructions using 0.5 criterion (Bottcher et al., 1997).

Structural Analysis

The visualization and segmentation of each of the structural components were performed with Amira (Mercury Computer Systems). The crystal structures of the P22 tailspike head binding domain (PDB ID: 1LKT) and distal receptor binding domain (PDB ID: 1TSP) were fitted independently into the corresponding density segments using *foldhunter* (Jiang et al., 2001) and the registration module in Amira. The movie of the asymmetric reconstruction was produced using the modules in SAIL (Dougherty and Chiu, 1998) based on IRIS Explorer visualization software.

Supplemental Data

Supplemental Data, including a movie showing the asymmetric reconstruction of bacteriophage P22, are available at <http://www.structure.org/cgi/content/full/14/6/1073/DC1/>.

Acknowledgments

We would like to thank Mr. Matthew Dougherty for generating the supplemental movie. We thank Dr. Steve Harvey at Georgia Institute of Technology for discussions on the dsDNA packaging model in phage particles. This research has been supported by grants from NIH (R01GM070557, R01AI38469, P41RR02250, and R01GM17980) and the Robert Welch Foundation.

Received: April 3, 2006

Accepted: May 9, 2006

Published online: May 24, 2006

References

- Agirrezabala, X., Martin-Benito, J., Caston, J.R., Miranda, R., Valpuesta, J.M., and Carrascosa, J.L. (2005). Maturation of phage T7 involves structural modification of both shell and inner core components. *EMBO J.* 24, 3820–3829.
- Andrews, D., Butler, J.S., Al-Bassam, J., Joss, L., Winn-Stapley, D.A., Casjens, S., and Cingolani, G. (2005). Bacteriophage P22 tail accessory factor GP26 is a long triple-stranded coiled-coil. *J. Biol. Chem.* 280, 5929–5933.
- Baker, M.L., Jiang, W., Rixon, F.J., and Chiu, W. (2005). Common ancestry of herpesviruses and tailed DNA bacteriophages. *J. Virol.* 79, 14967–14970.
- Bamford, D.H., Grimes, J.M., and Stuart, D.I. (2005). What does structure tell us about virus evolution? *Curr. Opin. Struct. Biol.* 15, 655–663.
- Bayer, M.E. (1968). Adsorption of bacteriophages to adhesions between wall and membrane of *Escherichia coli*. *J. Virol.* 2, 346–356.
- Bazinet, C., and King, J. (1988). Initiation of P22 procapsid assembly in vivo. *J. Mol. Biol.* 202, 77–86.
- Bazinet, C., Benbasat, J., King, J., Carazo, J.M., and Carrascosa, J.L. (1988). Purification and organization of the gene 1 portal protein required for phage P22 DNA packaging. *Biochemistry* 27, 1849–1856.
- Booth, C.R., Jiang, W., Baker, M.L., Zhou, Z.H., Ludtke, S.J., and Chiu, W. (2004). A 9 Å single particle reconstruction from CCD captured images on a 200 kV electron cryomicroscope. *J. Struct. Biol.* 147, 116–127.
- Botstein, D., Waddell, C.H., and King, J. (1973). Mechanism of head assembly and DNA encapsulation in *Salmonella* phage p22. I. Genes, proteins, structures and DNA maturation. *J. Mol. Biol.* 80, 669–695.
- Bottcher, B., Wynne, S.A., and Crowther, R.A. (1997). Determination of the fold of the core protein of hepatitis B virus by electron cryomicroscopy. *Nature* 386, 88–91.
- Bryant, J.L., Jr., and King, J. (1984). DNA injection proteins are targets of acridine-sensitized photoinactivation of bacteriophage P22. *J. Mol. Biol.* 180, 837–863.
- Casjens, S., and Hayden, M. (1988). Analysis in vivo of the bacteriophage P22 headful nuclease. *J. Mol. Biol.* 199, 467–474.
- Casjens, S., and Weigele, P. (2005). DNA packaging by bacteriophage P22. In *Viral Genome Packaging Machines: Genetics, Structure, and Mechanism*, C.E. Catalano, ed. (Georgetown, TX; New York: Landes Bioscience/Eurekah.com; Kluwer Academic/Plenum Publishers), pp. 80–88.
- Casjens, S., Sampson, L., Randall, S., Eppler, K., Wu, H., Petri, J.B., and Schmieger, H. (1992a). Molecular genetic analysis of bacteriophage P22 gene 3 product, a protein involved in the initiation of headful DNA packaging. *J. Mol. Biol.* 227, 1086–1099.
- Casjens, S., Wyckoff, E., Hayden, M., Sampson, L., Eppler, K., Randall, S., Moreno, E.T., and Serwer, P. (1992b). Bacteriophage P22 portal protein is part of the gauge that regulates packing density of intravirion DNA. *J. Mol. Biol.* 224, 1055–1074.
- Cerritelli, M.E., Cheng, N., Rosenberg, A.H., McPherson, C.E., Booy, F.P., and Steven, A.C. (1997). Encapsidated conformation of bacteriophage T7 DNA. *Cell* 91, 271–280.
- Chen, B., and King, J. (1991). Thermal unfolding pathway for the thermostable P22 tailspike endorhamnosidase. *Biochemistry* 30, 6260–6269.
- Cingolani, G., Moore, S.D., Prevelige, P.E., Jr., and Johnson, J.E. (2002). Preliminary crystallographic analysis of the bacteriophage P22 portal protein. *J. Struct. Biol.* 139, 46–54.
- Dokland, T., and Murialdo, H. (1993). Structural transitions during maturation of bacteriophage lambda capsids. *J. Mol. Biol.* 233, 682–694.
- Dokland, T., Lindqvist, B.H., and Fuller, S.D. (1992). Image reconstruction from cryo-electron micrographs reveals the morphopoietic mechanism in the P2–P4 bacteriophage system. *EMBO J.* 11, 839–846.
- Dougherty, M.T., and Chiu, W. (1998). Using animation to enhance 3D visualization: a strategy for a production and environment. *Microsc. Microanal.* 4, 452–453.
- Droge, A., Santos, M.A., Stiege, A.C., Alonso, J.C., Lurz, R., Trautner, T.A., and Tavares, P. (2000). Shape and DNA packaging activity of bacteriophage SPP1 procapsid: protein components and interactions during assembly. *J. Mol. Biol.* 296, 117–132.
- Earnshaw, W.C., and Harrison, S.C. (1977). DNA arrangement in isometric phage heads. *Nature* 268, 598–602.
- Greene, B., and King, J. (1996). Scaffolding mutants identifying domains required for P22 procapsid assembly and maturation. *Virology* 225, 82–96.
- Harauz, G., and van Heel, M. (1986). Exact filters for general geometry three dimensional reconstruction. *Optik* 73, 146–156.
- Hartwig, E., Bazinet, C., and King, J. (1986). DNA injection apparatus of phage P22. *Biophys. J.* 49, 24–26.
- Hoffman, B., and Levine, M. (1975a). Bacteriophage P22 virion protein which performs an essential early function. I. Analysis of 16-ts mutants. *J. Virol.* 16, 1536–1546.
- Hoffman, B., and Levine, M. (1975b). Bacteriophage P22 virion protein which performs an essential early function. II. Characterization of the gene 16 function. *J. Virol.* 16, 1547–1559.
- Israel, V., Rosen, H., and Levine, M. (1972). Binding of bacteriophage-P22 tail parts to cells. *J. Virol.* 10, 1152–1158.
- Iwashita, S., and Kanegasa, S. (1973). Smooth specific phage adsorption: endorhamnosidase activity of tail parts of P22. *Biochem. Biophys. Res. Commun.* 55, 403–409.
- Jardine, P.J., and Anderson, D.L. (2006). DNA packaging in double-stranded DNA phages. In *The Bacteriophages*, R. Calendar, ed. (Oxford: Oxford University Press), pp. 49–65.
- Jiang, W., Baker, M.L., Ludtke, S.J., and Chiu, W. (2001). Bridging the information gap: computational tools for intermediate resolution structure interpretation. *J. Mol. Biol.* 308, 1033–1044.
- Jiang, W., Li, Z., Zhang, Z., Baker, M.L., Prevelige, P.E., Jr., and Chiu, W. (2003). Coat protein fold and maturation transition of bacteriophage P22 seen at subnanometer resolutions. *Nat. Struct. Biol.* 10, 131–135.
- Jiang, W., Chang, J., Jakana, J., Weigele, P., King, J., and Chiu, W. (2006). Structure of epsilon15 bacteriophage reveals genome organization and DNA packaging/injection apparatus. *Nature* 439, 612–616.
- Kanamaru, S., Leiman, P.G., Kostyuchenko, V.A., Chipman, P.R., Mesyanzhinov, V.V., Arisaka, F., and Rossmann, M.G. (2002). Structure of the cell-puncturing device of bacteriophage T4. *Nature* 415, 553–557.
- Kemp, P., Garcia, L.R., and Molineux, I.J. (2005). Changes in bacteriophage T7 virion structure at the initiation of infection. *Virology* 340, 307–317.
- King, J., and Casjens, S. (1974). Catalytic head assembling protein in virus morphogenesis. *Nature* 251, 112–119.
- King, J., Lenk, E.V., and Botstein, D. (1973). Mechanism of head assembly and DNA encapsulation in *Salmonella* phage P22. II. Morphogenetic pathway. *J. Mol. Biol.* 80, 697–731.
- King, J., Botstein, D., Casjens, S., Earnshaw, W., Harrison, S., and Lenk, E. (1976). Structure and assembly of the capsid of bacteriophage P22. *Philos. Trans. R. Soc. Lond. B Biol. Sci.* 276, 37–49.

- Kivioja, T., Ravantti, J., Verkhovsky, A., Ukkonen, E., and Bamford, D. (2000). Local average intensity-based method for identifying spherical particles in electron micrographs. *J. Struct. Biol.* **131**, 126–134.
- Ludtke, S.J., Baldwin, P.R., and Chiu, W. (1999). EMAN: semiautomated software for high-resolution single-particle reconstructions. *J. Struct. Biol.* **128**, 82–97.
- Ludtke, S.J., Nason, L., Tu, H., Peng, L., and Chiu, W. (2003). Object oriented database and electronic notebook for transmission electron microscopy. *Microsc. Microanal.* **9**, 556–565.
- McConnell, M., Walker, B., Middleton, P., Chase, J., Owens, J., Hyatt, D., Gutierrez, H., Williams, M., Hambright, D., Barry, M., Jr., et al. (1992). Restriction endonuclease and genetic mapping studies indicate that the vegetative genome of the temperate, Salmonella-specific bacteriophage, epsilon 15, is circularly-permuted. *Arch. Virol.* **123**, 215–221.
- Moak, M., and Molineux, I.J. (2004). Peptidoglycan hydrolytic activities associated with bacteriophage virions. *Mol. Microbiol.* **51**, 1169–1183.
- Orlova, E.V., Gowen, B., Droge, A., Stiege, A., Weise, F., Lurz, R., van Heel, M., and Tavares, P. (2003). Structure of a viral DNA gatekeeper at 10 Å resolution by cryo-electron microscopy. *EMBO J.* **22**, 1255–1262.
- Plancon, L., Chami, M., and Letellier, L. (1997). Reconstitution of FhuA, an Escherichia coli outer membrane protein, into liposomes. Binding of phage T5 to FhuA triggers the transfer of DNA into the proteoliposomes. *J. Biol. Chem.* **272**, 16868–16872.
- Poteete, A.R., and King, J. (1977). Functions of two new genes in Salmonella phage P22 assembly. *Virology* **76**, 725–739.
- Prasad, B.V., Prevelige, P.E., Marietta, E., Chen, R.O., Thomas, D., King, J., and Chiu, W. (1993). Three-dimensional transformation of capsids associated with genome packaging in a bacterial virus. *J. Mol. Biol.* **231**, 65–74.
- Prevelige, P.E. (2006). Bacteriophage P22. In *The Bacteriophages*, R. Calendar, ed. (Oxford: Oxford University Press), pp. 457–468.
- Prevelige, P.E., Jr., Thomas, D., and King, J. (1988). Scaffolding protein regulates the polymerization of P22 coat subunits into icosahedral shells in vitro. *J. Mol. Biol.* **202**, 743–757.
- Rixon, F.J., and Chiu, W. (2003). Studying large viruses. *Adv. Protein Chem.* **64**, 379–408.
- Roessner, C.A., Struck, D.K., and Ihler, G.M. (1983). Injection of DNA into liposomes by bacteriophage lambda. *J. Biol. Chem.* **258**, 643–648.
- Simpson, A.A., Tao, Y., Leiman, P.G., Badasso, M.O., He, Y., Jardine, P.J., Olson, N.H., Morais, M.C., Grimes, S., Anderson, D.L., et al. (2000). Structure of the bacteriophage phi29 DNA packaging motor. *Nature* **408**, 745–750.
- Smith, D.E., Tans, S.J., Smith, S.B., Grimes, S., Anderson, D.L., and Bustamante, C. (2001). The bacteriophage straight phi29 portal motor can package DNA against a large internal force. *Nature* **413**, 748–752.
- Steinbacher, S., Seckler, R., Miller, S., Steipe, B., Huber, R., and Reinemer, P. (1994). Crystal structure of P22 tailspike protein: interdigitated subunits in a thermostable trimer. *Science* **265**, 383–386.
- Steinbacher, S., Miller, S., Baxa, U., Budisa, N., Weintraub, A., Seckler, R., and Huber, R. (1997). Phage P22 tailspike protein: crystal structure of the head-binding domain at 2.3 Å, fully refined structure of the endorhamnosidase at 1.56 Å resolution, and the molecular basis of O-antigen recognition and cleavage. *J. Mol. Biol.* **267**, 865–880.
- Steven, A.C., Serwer, P., Bisher, M.E., and Trus, B.L. (1983). Molecular architecture of bacteriophage T7 capsid. *Virology* **124**, 109–120.
- Steven, A.C., Trus, B.L., Maizel, J.V., Unser, M., Parry, D.A., Wall, J.S., Hainfeld, J.F., and Studier, F.W. (1988). Molecular substructure of a viral receptor-recognition protein. The gp17 tail-fiber of bacteriophage T7. *J. Mol. Biol.* **200**, 351–365.
- Strauss, H., and King, J. (1984). Steps in the stabilization of newly packaged DNA during phage P22 morphogenesis. *J. Mol. Biol.* **172**, 523–543.
- Stummeyer, K., Dickmanns, A., Muhlenhoff, M., Gerardy-Schahn, R., and Ficner, R. (2005). Crystal structure of the polysialic acid-degrading endosialidase of bacteriophage K1F. *Nat. Struct. Mol. Biol.* **12**, 90–96.
- Tang, L., Marion, W.R., Cingolani, G., Prevelige, P.E., and Johnson, J.E. (2005). Three-dimensional structure of the bacteriophage P22 tail machine. *EMBO J.* **24**, 2087–2095.
- Thuman-Commike, P.A., Greene, B., Jakana, J., Prasad, B.V., King, J., Prevelige, P.E., Jr., and Chiu, W. (1996). Three-dimensional structure of scaffolding-containing phage p22 procapsids by electron cryo-microscopy. *J. Mol. Biol.* **260**, 85–98.
- Thuman-Commike, P.A., Tsuruta, H., Greene, B., Prevelige, P.E., Jr., King, J., and Chiu, W. (1999). Solution x-ray scattering-based estimation of electron cryomicroscopy imaging parameters for reconstruction of virus particles. *Biophys. J.* **76**, 2249–2261.
- Trus, B.L., Cheng, N., Newcomb, W.W., Homa, F.L., Brown, J.C., and Steven, A.C. (2004). Structure and polymorphism of the UL6 portal protein of herpes simplex virus type 1. *J. Virol.* **78**, 12668–12671.
- Weigele, P.R., Sampson, L., Winn-Stapley, D., and Casjens, S.R. (2005). Molecular genetics of bacteriophage P22 scaffolding protein's functional domains. *J. Mol. Biol.* **348**, 831–844.
- Whitfield, C. (1995). Biosynthesis of lipopolysaccharide O antigens. *Trends Microbiol.* **3**, 178–185.
- Wikoff, W.R., Liljas, L., Duda, R.L., Tsuruta, H., Hendrix, R.W., and Johnson, J.E. (2000). Topologically linked protein rings in the bacteriophage HK97 capsid. *Science* **289**, 2129–2133.
- Zhang, Z., Greene, B., Thuman-Commike, P.A., Jakana, J., Prevelige, P.E., Jr., King, J., and Chiu, W. (2000). Visualization of the maturation transition in bacteriophage P22 by electron cryomicroscopy. *J. Mol. Biol.* **297**, 615–626.

Accession Numbers

The 3D density map has been deposited to the EBI database with accession number EMD-1222.